

Quantum dual-path interferometry scheme for axion dark matter searches

Qiaoli Yang^{1,*}, Yu Gao^{2,†} and Zhihui Peng^{3‡}

¹*Department of Physics and Siyuan Laboratory,*

Jinan University,

Guangzhou 510632, China

²*Key Laboratory of Particle Astrophysics,*

Institute of High Energy Physics,

Chinese Academy of Sciences,

Beijing 100049, China

³*Key Laboratory of Low-Dimensional Quantum Structures*

and Quantum Control of Ministry of Education,

Key Laboratory for Matter Microstructure and Function of Hunan Province,

Department of Physics and Synergetic Innovation

Center for Quantum Effects and Applications,

Hunan Normal University,

Changsha 410081, China

Abstract

We propose a dual-path interferometry amplification configuration in the cavity axion dark matter searches. We show quantum-mechanically that, in a low temperature cavity permeated by a magnetic field, the single axion-photon conversion rate is enhanced by the cavity quality factor Q , and quantitatively larger than the classical result by a factor $\pi/2$. Under modern cryogenic conditions, thermal photons in the cavity are negligible, thus the axion cavity can be considered as a quantum device emitting single-photons with temporal separations. This differs from the classical picture in which axions transition in batches and the converted energy accumulates in the electromagnetic field inside the cavity. It reveals a possibility for the axion cavity experiment to handle the signal sensitivity at the quantum level, e.g. cross-power and second order correlation measurements. The correlation of photon field quadratures in the amplification chain, within current technology, enhances the signal-to-noise ratio up to two orders of magnitude or one order of magnitude compared with single-path amplification scheme based on high electronic mobility transistor amplifier or Josephson Parametric Amplifiers (JPA), respectively. Especially, it is useful to combine the dual-path interferometry scheme with other techniques, e.g. JPAs, to overcome the inevitable microwave signals insertion loss (normally it is ~ -3 dB) in the channels between the cavity and the quantum-limited amplifiers. This enhancement would greatly reduce the signal scanning time and improve the sensitivity of the axion-photon coupling. In addition, the second order correlation function measurement in the due path scheme can provide an additional verification that if the candidate signals are axion converted or other noises.

PACS numbers:

The existence of cold dark matter is widely accepted [1] and one promising candidate is the axion [2–14]. The axion is a natural extension of the Standard Model of particle physics in which the amount of Charge-Parity violation by the strong interaction is determined by the vacuum angle whose value should be order one. However, experiments measuring the neutron electric dipole moment [15] suggest an essentially vanishing vacuum angle [16], thus

^{*}Electronic address: qiaoliyang@jnu.edu.cn

[†]Electronic address: gaoyu@ihep.ac.cn

[‡]Electronic address: zhihui.peng@hunnu.edu.cn

give rise to a puzzle known as the strong-CP problem [17, 18]. The problem could be solved by adding the Peccei-Quinn (PQ) symmetry [2, 3] which must be spontaneously broken by a PQ preserving potential and explicitly broken by the QCD instanton effect [19, 20]. The symmetry breaking implies the existence of a pseudo Nambu-Goldstone boson which is called [14] the QCD axion and currently there are two QCD axion benchmark models, the KSVZ [6, 7] and the DFSZ [8, 9] models. The cosmic axions can be produced abundantly during the QCD phase transition in the early universe and their relic composes the cold dark matter observed today [10–13]. Depending on the scenario whether the PQ symmetry happened before or after the cosmological inflation, the natural mass window of the QCD axions being majority of dark matter is about $\mathcal{O}(10^{-5} - 10^{-3})$ eV [21] or $< \mathcal{O}(10^{-7})$ eV [22], but other production mechanisms are possible which will lead to wider mass ranges. The axion couples to the Standard Model particles weakly, in particular, it couples to two photons with a coupling $\mathcal{O}(10^{-17} - 10^{-12})$ GeV $^{-1}$ depending on the PQ scale. Currently many proposed and ongoing experimental studies such as [23–30] and others are actively searching dark matter axions. Interestingly, in condensed-matter systems quasi-particle "axions" could lead to many exciting physical phenomena [31–36] etc., it is tempting to believe that nature has repeated itself in many different levels.

Axion haloscope experiments are based on Sikivie's resonant cavity design [37] in which the cosmic axions resonantly convert into a microwave signal in a high- Q cavity permeated by a magnetic field. Although the axion-photon coupling is small, the conversion rate is enhanced by the coherence of the axion field, the magnitude of the magnetic field, and the high- Q of the cavity. The modern cryogenic technology can sustain $\mathcal{O}(20)$ mK or lower temperature, which results in a sub-unity thermal photon occupation number $\bar{n} \sim 10^{-5}$ at the resonant frequency (typically at several GHz) in the cavity. Therefore, it is useful to consider the quantum transition picture in the cavity especially at such low photon occupation number. We find that the Q factor enhances the axion-photon transition at quantum level and that could be used to facilitate the dark matter axion searches.

In this letter, we propose using a 50/50 beam splitter followed by the linear amplifiers or detectors to construct a dual-path measurement scheme that realizes Hanbury Brown and Twiss (HBT) interferometry [38] in quantum optics. The linear detectors (phase-preserving amplifiers) are widely used in the axion haloscope experiments. Current commercial cryogenic high electron mobility transistor (HEMT) [39] already offers a flat gain over a frequency

range of 10 GHz with an adding random noise at 10-20 photons [39], and amplifiers like the Josephson Parametric Amplifier (JPA) [40] can approach to the quantum limit. At very low signal/thermal photon occupation numbers, the major sensitivity hurdles are due to the quantum fluctuations and the added noises in detection channel. The general method of signal identification is to accumulate sufficient statistics at each giving frequency point so it takes a very long integration time due to the unfavorable signal-to-noise ratio. The interferometer scheme in microwave quantum optics, however, has already demonstrated to achieve *two orders of magnitude* noise reduction [41–44], as the un-correlated noises in the dual receiver chains cancel and the correlations of field quadratures can be measured. With this scheme, the effective correlated noise level can be significantly lower than the noise level in a single amplification channel because the interferometer scheme is not sensitive to the inevitable microwave signals insertion loss in the channels between the cavity and the amplifiers.

Axion cavity at quantum level: The QCD axion was proposed to solve the Strong CP problem. Its couplings to the standard model particles cannot be arbitrarily weak otherwise the axions would be overproduced in the early universe. Nevertheless, the viable “invisible axion” models give rise to extremely weak couplings and very light masses that hinder the axion experimental searches. Fortunately, the dark matter axion production mechanism [10–13] gives hints to a preferred axion mass window around neV, although the uncertainty could be several orders of magnitude. Various dark matter axion search methods aiming at this mass window have been proposed. In these proposals, the axion cavity haloscopes are particularly sensitive and are the only experiments that can reach the QCD axion parameter space up to now. The original calculation was given in[37, 45] in a picture that the cavity captures the photons produced and enhances the conversion process through resonance when one of the cavity modes matches the energy of axion signal. However, it was uncertain if the transition rate can be enhanced during a single axion-photon conversion, which is quantum in nature. Some calculations, e.g. Ref. [46] applied the Feynman diagram method which requires existing of asymptotic outgoing states, thus can not derive the resonant cavity’s enhancement and form factor etc..

The axion field a couples to the photons by

$$\mathcal{L}_{a\gamma\gamma} = -g_{a\gamma\gamma} a \vec{E} \cdot \vec{B} \quad , \quad (1)$$

where the axion-photon coupling $g_{a\gamma\gamma}$ is defined as $g_{a\gamma\gamma} = c_\gamma\alpha/(\pi f_a)$, f_a is the PQ scale factor, $\alpha = 1/137$ is the fine-structure constant and c_γ is a model-dependent factor order of one.

The present day axion dark matter halo profile is crucial to the axion searches, but luckily there are only two important factors for current discussion: (i) the dark matter halo has a local density $\rho_a = \rho_{CDM} \approx 0.45 \text{ GeV/cm}^3$; (ii) the axion dark matter is highly coherent which is a consequence of the small axion mass m_a and their slow velocity $v_a \sim 10^{-3}c$ in the halo.

Due to the small axion mass and the low velocity, the axion dark matter has a long de-Broglie wavelength $\lambda_a = 2\pi/(m_a v) \sim \mathcal{O}(1 - 100)$ meters, much larger than the size of a respective resonant cavity so the axion field is homogeneous in a haloscope cavity. In addition, the axion coherent time $\tau_a = \lambda_a/\delta v_a \sim 2\pi/(m_a v_a^2)$ is also significantly longer than the photon existing time in the cavity: $\tau_c = 2\pi Q/\omega_a \approx 2\pi Q/m_a$, where $Q \sim 10^5$ for current state of the art technology, thus the axion field can be regarded as monochromatic during a cavity model transition (Notice that in some axion halo models the coherent time could be even longer if $\delta v_a \ll v_a$ [47, 48]). Thus we can write the axion field as

$$a \approx a_0 \cos(\omega_a t) = \frac{\sqrt{2\rho_a}}{m_a} \cos(\omega_a t) . \quad (2)$$

In experimental literatures axion quality factor $Q_a = 1/v_a^2 \sim 10^6$ is often used to describe coherence of axions.

In a cavity, the electric field operator \vec{E} can be expanded as

$$\vec{E} = i \sum \sqrt{\frac{\omega_k}{2}} [a_k \vec{U}_k(\vec{r}) e^{-i\omega_k t} - a_k^\dagger \vec{U}_k^*(\vec{r}) e^{i\omega_k t}] , \quad (3)$$

where a_k , and a_k^\dagger are the annihilation and creation operators for the photon Fock state respectively, $\vec{U}_k(\vec{r})$ is the cavity modes satisfying the wave equation $(\nabla^2 + \omega_k^2) \vec{U}_k(\vec{r}) = 0$ with cavity-wall boundary conditions, and k denotes different cavity modes. Assuming the permitted magnetic field is along the \hat{z} direction, $\vec{B} = \hat{z}B_0$, the interaction Hamiltonian can be written as

$$\begin{aligned} H_I &= - \int d^3x \mathcal{L}_{a\gamma\gamma} \\ &= \left(g_{a\gamma\gamma} \frac{\sqrt{2\rho_a}}{m_a} B_0 \int d^3x \hat{z} \cdot \vec{E} \right) \cos(\omega_a t) . \end{aligned} \quad (4)$$

Up to the first order, the photon $|0\rangle \rightarrow |1\rangle$ transition probability is

$$\begin{aligned}
P &\approx \left| \langle 1 | \int_0^t dt H_I | 0 \rangle \right|^2 \\
&\approx g_{a\gamma\gamma}^2 \frac{\rho_a}{m_a^2} B_0^2 \sum_k \omega_k \left| \int d^3x \hat{z} \cdot \vec{U}_k^* \right|^2 \\
&\times \frac{\sin^2[(\omega_k - \omega_a)t/2]}{4[(\omega_k - \omega_a)/2]^2} .
\end{aligned} \tag{5}$$

When t is large, we can use the approximation $\sin^2(\Delta\omega t/2)/[\Delta\omega/2]^2 \approx 2\pi t\delta(\Delta\omega)$. The transition rate is $R = dP/dt$. Let us define the form factor

$$C_k = \frac{\left| \int d^3x \hat{z} \cdot \vec{U}_k \right|^2}{V \int d^3x |\vec{U}_k|^2} , \tag{6}$$

where V is the volume of the cavity, and the factor $\int d^3x |\vec{U}_k|^2$ properly normalizes the photon field operator. Then we have

$$R \approx \frac{\pi}{2} g_{a\gamma\gamma}^2 \frac{\rho_a}{m_a^2} B_0^2 V \sum_k C_k \omega_k \delta(\omega_k - \omega_a) . \tag{7}$$

Since $\sum C_k \omega_k \delta(\omega_k - \omega_a) \approx \int C_k d\omega (\omega/d\omega) \delta(\omega - \omega_a) \approx Q C_{\omega_a}$, we have the transition rate

$$R \approx \frac{\pi}{2} g_{a\gamma\gamma}^2 \frac{\rho_a}{m_a^2} B_0^2 C_{\omega_a} V Q . \tag{8}$$

This shows the single axion-photon transition power $P_{sig} = \omega_a R \approx m_a R$ is *enhanced* by the cavity's quality factor Q , and it is in good agreement with calculations in the classical picture. For a typical haloscope setup, the cavity volume is about a liter, with $Q \sim 10^5$ and $B \sim 10$ T magnetic field, the $a \rightarrow \gamma$ conversion rate is about $\mathcal{O}(1)$ per second for the QCD axions, thus the signal temporal separations far exceed the resolution of linear detectors.

The thermal photon occupation number in the cavity is

$$n(\omega_a, T) = \frac{1}{e^{\omega_a/k_B T} - 1} . \tag{9}$$

For axion mass $m_a \geq 10^{-5}$ eV and a cavity operating around $T \approx 20$ mK, the thermal photon state has a low occupation number $n \ll 1$, thus the cavity is almost always in the vacuum state. It is convenient to define the cavity coupling parameter $\beta = Q_0/Q_c$, where Q_0 is the quality factor due to the photon losses by cavity-wall absorption and Q_c is due to the photons leaving the cavity. The combined quality factor is then $Q^{-1} = Q_0^{-1} + Q_c^{-1}$ and the

photon emitting rate is $R \cdot \beta/(1 + \beta)$. Ideally $\beta \sim 1$ is the optimal working point but its exact value depends on the cavity designs. In summary, the axion cavity can be regarded as a single photon emitter with a slow rate $R \lesssim 10$ Hz.

Dual-path interferometry: Since the axion cavity is a single photon emitter at low pulse rates, the major experimental bottleneck lies in the detection sensitivity to weak microwave signals at the single-photon level. So far, practical microwave single-photon detectors are still yet to realize, mainly because the microwave photon energy is several orders of magnitude lower than that of an optic photon, resulting in detection difficulty of microwave single photons [49]. Currently, a typical linear detector scheme for axion cavity search consists of an amplification chain, which is a cryogenic HEMT amplifier as a pre-amplifier placing at 4 K temperature stage in a dilution refrigerator, and subsequent room-temperature amplifiers. The amplified microwave signal at GHz would be down-converted to few tens of MHz, and then sampled by digitizers at room temperature. The typical noise temperature of cryogenic HEMT is around several Kelvin. Considering the loss in channel from microwave signal emitted from cavity at 20 mK stage to the cryogenic HEMT placing at 4 K stage in refrigerator, the effective noise temperature T_{eff} in detection channel could be higher than 10 K.

Thus the effective temperature T_{eff} on readout is often much higher than the physical temperature in the cavity. The signal-to-noise ratio is

$$\text{SNR} = \frac{P_{sig}}{k_B T_{eff}} \sqrt{\frac{t}{b}} , \quad (10)$$

where b is the detection bandwidth, P_{sig} is the signal power, k_B is the Boltzmann constant and t is the integration time. The sensitivity on $g_{a\gamma\gamma}^2$ is inversely proportional to T_{eff} , or grows over the square-root of integrated time. With the development of superconducting quantum information technology, recent axion cavity experiments, like ADMX-Sidecar [50], QUAX- $a\gamma$ [51], etc. have applied JPAs with performance approaching to the quantum limit. However, the detector performance is restricted by quantum fluctuations and there are around ~ -3 dB insertion loss from coaxial cables, switchers and circulators mounted between the cavity and the quantum-limited amplifiers. The effective noise temperature of detection channel is at least twice higher than the Standard Quantum Limit(SQL).

Here we briefly interpret the quantum noise with detector observables,

$$\hat{I}_r \cos(\omega_a t) + \hat{Q}_r \sin(\omega_a t) = \text{Re} \left((\hat{I}_r + i\hat{Q}_r) e^{i\omega_a t} \right) . \quad (11)$$

Where, we define the in-phase \hat{I}_r and quadrature \hat{Q}_r component operators with $\hat{I}_r = (\hat{r}^\dagger + \hat{r})/2$, $\hat{Q}_r = -i(\hat{r}^\dagger - \hat{r})/2$ using the creation and annihilation operators \hat{r}^+ and \hat{r} . These operators satisfy commutation relations

$$[\hat{I}_r, \hat{Q}_r] = i/2 \text{ and } [\hat{r}^+, \hat{r}] = 1 . \quad (12)$$

Assuming the linear detector enhances the field by a gain of G , we have

$$\frac{\hbar\omega_a}{2} + \frac{(G^2 - 1)\hbar\omega_a}{2G^2} \approx \hbar\omega_a, \quad (13)$$

and for a large G this is often called the SQL [52]. To protect the cavity at 20 mK from the thermal noise leakage from the second stage amplifier (e.g. cryogenic HEMT at 4 K), it requires pre-amplifier gain over 20 dB. To the best of our knowledge, it is still difficult to achieve 20dB gain over a 1 GHz bandwidth for a JPA or a Traveling-Wave Parametric Amplifier (TWPA) [53], with the added noise photon approaching half quantum of noise to the input signal simultaneously.

For signals with quantum origin, a dual-path measurement can be a powerful tool as it measures the statistical correlation between quadratures in the two channels in addition to the photon number $n = \langle a^\dagger a \rangle$ in each channel. Recent quantum optics developments enable dual-path detection in the microwave-frequency domain, and it can be performed with phase-preserving linear amplifiers as well [41–44, 54]. Linear amplifiers are well-known for their high signal gain for weak electromagnetic field signals, yet at the cost of extra noise. With a 50/50 beam splitter, as shown in Fig. 1, dual linear amplifier chains can be constructed to measure the signal correlation information. It has been shown [41, 42, 44] that with a recording of the full time traces of the signals in both channels instead of the time-averaged value in a single, the signal's cross power in two channels can be extracted and significant improves the SNR.

The dual-path scheme in Fig. 1(a) forms a Hanbury Brown-Twiss interferometer set-up. The axion cavity acts as a quantum emitter to inject microwave single-photon field \hat{r} , which passes through a microwave-frequency beam splitter. The beam splitter gives rise to two output fields in channel 1 and 2,

$$\hat{r}_1 = (\hat{r} + \hat{\nu}_m)/\sqrt{2} \text{ and } \hat{r}_2 = (\hat{r} - \hat{\nu}_m)/\sqrt{2} . \quad (14)$$

$\hat{\nu}_m$ is added noise field, for instance, $\hat{\nu}_m$ as the vacuum state or a weak thermal state. Then, by measuring $\hat{I}_1 = (\hat{r}_1 + \hat{r}_1^+)/2$ and $\hat{Q}_2 = -i(\hat{r}_2 - \hat{r}_2^+)/2$, a complex observable can be

constructed as,

$$\hat{S}_a(t) = I_1(t) + iQ_2(t) = \hat{r} + \hat{\nu}_m^+ . \quad (15)$$

In fact, $\hat{S}_a(t)$ behaves classically and resembles a complex number because $\hat{S}_a^+ = \hat{S}_a^*$ and $[\hat{S}_a^+, \hat{S}_a] = 0$ under the effect of the added noise ν_m [55]. After amplification and mixing, the two classical complex envelopes $S_i(t)$, $i = 1, 2$, at digitizers can be written as

$$S_i(t) = G_i \hat{r}(t) + \sqrt{G_i^2 - 1} h_i^+(t) + \nu_{m,i}^+(t) , \quad (16)$$

here we let h_i denote for the added thermal noise in each linear amplifier chain, and $\nu_{m,i}(t)$ for the vacuum noise. Both quadratures of \hat{S}_i can be measured simultaneously by digitizers due to the commutator $[\hat{S}_i, \hat{S}_i^+] = 0$. Powerful FPGA (Field Programmable Gate Array) [41, 42] or GPU (Graphics Processing Unit) [44] can analyse the correlation of field quadratures in real-time. The correlations of output field quadratures are constructed as

$$\langle (S_i^*)^m S_j^n \rangle = \langle (S_i^+)^m S_j^n \rangle = \langle (\hat{r}^+)^m \hat{r}^n \rangle , \quad (17)$$

with integer-number power indexes m and n .

Sensitivity enhancement: It is now straightforward to show that the signal can be picked up by the instantaneous power function $\langle S_i^*(t) S_j(t) \rangle$, where the *power* is

$$\langle S_i^*(t) S_i(t) \rangle = G_i^2 (\langle \hat{r}^+(t) \hat{r}(t) \rangle + N_i + 1) , \quad (18)$$

and the *cross-power* is

$$\langle S_1^*(t) S_2(t) \rangle = G_1 G_2 (\langle \hat{r}^+(t) \hat{r}(t) \rangle + N_{12}) , \quad (19)$$

respectively. Here, the component $P_{\text{cavity}} = \langle \hat{r}^+(t) \hat{r}(t) \rangle$ identifies with the power from the cavity, $N_i = (G_i^2 - 1) \langle h_i^+ h_i \rangle / G_i^2$ is the power of noise in single channel, and $N_{12} = \sqrt{(G_1^2 - 1)(G_2^2 - 1)} \langle h_1 h_2^+ \rangle / G_1 G_2$ is the power of correlated noise between channel 1 and 2. $\langle h_1 h_2^+ \rangle \sim 0$ because the two noise modes in the two detection channels are commutable and mostly uncorrelated. That is

$$N_{12} \ll N_i + 1 , \quad (20)$$

significantly lower than the magnitude of a single path noise, as illustrated in Fig 2. Notely, the minimum of $N_i + 1$ is related to the noise set by SQL. We emphasize that it is crucial to upgrade from the traditional single-path setup to *dual-path* in order to cancel the main part

of uncorrelated noises from different detection channels. In practice, the scale of remaining correlated noise N_{12} depends on the experimental devices and it can be directly measured by the cross power without an axion cavity. It can be explained by the thermal leakage from cryogenic HEMT at 4 K and induced the correlated noise between two channels of beam splitter. Actually, it has demonstrated that the correlated noise N_{12} can be reduced and the SNR can be enhanced for the cross-power measurement if there are quantum isolators or JPAs between beam splitter and HEMT at 4 K [54].

The pre-amplifiers or detectors can be placed at distance from the cavity output port to help shield the strong magnetic field. The insertion loss is inevitable because there are a series of microwave coaxial cables, switchers and circulators between the cavity's port and the pre-amplifiers/detectors. In realistic experiments, for instance, the effective noise temperature in the detection channel is ~ 925 mK at 4.798 GHz even by using JPA with a insertion loss ~ -3 dB [50]. However, the effective noise temperature should be ~ 240 mK if it is only limited by the SQL. Therefore, there is an obvious advantage to use dual-path interferometer scheme which can approaching the effective noise temperature with ~ 120 mK which is come from quantum vacuum fluctuations, especially to use two-sided cavity scheme described in Fig.1(b) to detect converted microwave single-photons signal. In the two-sided cavity dual-path scheme, there are two identical output ports and the converted microwave single-photons escape from them with equal probability. The correlations between the two cavity outputs behave like to the outputs of the beam splitter in Fig. 1(a). The dual-path interferometer is not sensitive to loss or thermal noise in the single channel, and the SNR could be enhanced one order magnitude compared with single-path amplification scheme based on JPA.

Recent dual-path setups [41–44] showed by using cross-power, the effective noise temperature could be reduced by two orders of magnitude compared to that of single channel. Fig. 2 illustrates the two order of magnitude noise level reduction with the simulation of cross-power between two channels and the power in one channel averaged over the same time. It has been demonstrated that in a dual-path experiment with cryogenic HEMT as pre-amplifiers, the effective correlated noise temperature is about 80 mK for dual-path setup, which is much smaller than the characteristic ~ 10 K noise in each detection chain [42] or by more than two orders of magnitude.

By Eq. 10, the SNR with a cross-power measurement is much higher than the power

calculation by replacing the SQL with a reduced effective noise temperature. This allows faster signal-significance accumulation and reduces the amount of required time-exposure at each frequency point in future cavity axion dark matter search, esp. at relative high frequencies. Actually, the assumption of the equal gain in both amplification channels and balanced microwave beam splitter is not difficult to achieve in experiment [41–44], and even unbalanced detection channel does not hinder the cancelation of correlated noises.

The second order correlation function measurement: Interestingly, for power correlation statistics one may consider

$$\begin{aligned} C^2(t, t + \tau) &= \langle \hat{r}^+(t) \hat{r}^+(t + \tau) \hat{r}(t + \tau) \hat{r}(t) \rangle \\ &= 4 \langle S_1^+(t) S_1^+(t + \tau) S_2(t + \tau) S_2(t) \rangle. \end{aligned} \quad (21)$$

As widely exploited in quantum optics, single-photon signals demonstrate two important features: sub-Poissonian statistics $C^2(\tau) \leq 1$ and photon anti-bunching $C^2(0) < C^2(\tau)$ [42–44, 54]. When a signal candidate emerges during a scan, the second-order function measurement, as simulated in Fig. 3, allows the measured $C^2(0)$ value to verify the nature of the signal: whether it is converted as a single-photon from dark matter axion ($C^2(0) \sim 0$), or simply from thermal noise ($C^2(0) \sim 1$). ($C^2(0) \sim 0$) arises from the fact that a single photon can only arrive at one path at one time, and it is a well-known technique in quantum optics to veto thermal noises [41–44]. Thus our dual-path scheme can provide an additional test of the signal’s nature when cavity’s predicted occupation numbers are small, in which case most axion-converted signals exit the cavity as single photons.

We have to emphasize that it is easy to combine the quantum dual-path scheme with other techniques, such as JPAs, microwave squeezing-state, and single-photon detector. Even with JPAs, the single-path noise temperature is around four times higher than that limited by the SQL [50]. However, with the dual-path measurement setup, the noise due to the SQL in single-path could be avoided. With squeezing-state, a fractional breaching of SQL has been achieved [56], while for cross-power at least an order of magnitude difference between correlated and uncorrelated noise level is typically expected [41–44]. In addition, both JPA and squeezing-state techniques have rather small working bandwidths compared that of cryogenics HEMT. It is also expected the effective noise temperature can be further lowered that by using JPA or TWPA as pre-amplifiers to protect the axion haloscope detector and beam splitter from thermal noise leaked from high temperature stage, e.g. HEMT at 4 K

[54]. It is proposed to detect axion by microwave single-photon detector [57]. We have to emphasize it is also easy to combine the dual-path measurement setup with single-photon detector and it is obvious can overcome the loss in the single-path detection channel as discussed earlier. It is expected a SNR of axion detection reach a limit from the temperature of axion haloscope cavity itself. We think the best way would be combine our dual-path scheme with broad-band, high-efficiency single-photon detectors to apply in axion search in future.

Summary: The axion cavity signal can be modeled quantum-mechanically at a low transition rate as a single photon Fock state in the cavity is populated and then quickly decayed. We show that the single-photon $a \rightarrow \gamma$ transition rate is amplified by the cavity Q -factor, consistent with the classical picture. Since the axion-cavity acts as a quantum signal emitter, it is very effective to employ the cross-power measurement in a dual-path interferometry setup instead of using a single channel receiver. The single-photon signal is slitted by a 50/50 beam splitter, then amplified and mixed by heterodyne detectors. With a digital analyzer, the measured cross-power effectively reduce the noise level due to the cancellation of uncorrelated noise in the two channels. Compared to the traditional single-channel readout, two order of magnitude enhancement in signal-noise ratio can be achieved with current dual-path setup with the HEMT as pre-amplifiers and one order of magnitude enhancement for JPA as pre-amplifiers. Furthermore, one can combine the dual-path interferometry scheme with other techniques, e.g. single-photon detectors, to approach the noise temperature limited by the temperature of axion haloscope cavity itself. Dual-path scheme can provide substantially faster scanning rate for the axion dark matter searches, or equivalently much higher sensitivity of the axion photon coupling. The second order correlation function measurement can provide a test of the single-photon nature of an axion-conversion signal.

Acknowledgments: Authors thank for helpful discussions with Lan Zhou, Yu-Xi Liu and Chang-Ling Zou. Q.Y. is supported by NSFC under Grant No. 11875148. Y.G. is partially supported by the National R&D Program of China, 2020YFC2201601. Z.P. is

supported by NSFC under Grant No. 61833010, No. 12074117 and No. 12061131011.

- [1] P. A. R. Ade et al. (Planck), *Astron. Astrophys.* **594**, A13 (2016), 1502.01589.
- [2] R. D. Peccei and H. R. Quinn, *Phys. Rev. Lett.* **38**, 1440 (1977), [,328(1977)].
- [3] R. D. Peccei and H. R. Quinn, *Phys. Rev.* **D16**, 1791 (1977).
- [4] S. Weinberg, *Phys. Rev. Lett.* **40**, 223 (1978).
- [5] F. Wilczek, *Phys. Rev. Lett.* **40**, 279 (1978).
- [6] J. E. Kim, *Phys. Rev. Lett.* **43**, 103 (1979).
- [7] M. A. Shifman, A. I. Vainshtein, and V. I. Zakharov, *Nucl. Phys.* **B166**, 493 (1980).
- [8] A. R. Zhitnitsky, *Sov. J. Nucl. Phys.* **31**, 260 (1980), [Yad. Fiz.31,497(1980)].
- [9] M. Dine, W. Fischler, and M. Srednicki, *Phys. Lett.* **104B**, 199 (1981).
- [10] J. Preskill, M. B. Wise, and F. Wilczek, *Phys. Lett.* **B120**, 127 (1983), [,URL(1982)].
- [11] L. F. Abbott and P. Sikivie, *Phys. Lett.* **B120**, 133 (1983), [,URL(1982)].
- [12] M. Dine and W. Fischler, *Phys. Lett.* **B120**, 137 (1983), [,URL(1982)].
- [13] P. Sikivie, *Phys. Rev. Lett.* **48**, 1156 (1982).
- [14] F. Wilczek (1991).
- [15] R. J. Crewther, P. Di Vecchia, G. Veneziano, and E. Witten, *Phys. Lett. B* **88**, 123 (1979), [Erratum: *Phys.Lett.B* 91, 487 (1980)].
- [16] C. A. Baker et al., *Phys. Rev. Lett.* **97**, 131801 (2006), hep-ex/0602020.
- [17] R. D. Peccei, *Lect. Notes Phys.* **741**, 3 (2008), hep-ph/0607268.
- [18] J. E. Kim and G. Carosi, *Rev. Mod. Phys.* **82**, 557 (2010), [Erratum: *Rev.Mod.Phys.* 91, 049902 (2019)], 0807.3125.
- [19] C. G. Callan, Jr., R. F. Dashen, and D. J. Gross, *Phys. Rev. D* **17**, 2717 (1978).
- [20] C. Vafa and E. Witten, *Phys. Rev. Lett.* **53**, 535 (1984).
- [21] P. Sikivie, *Lect. Notes Phys.* **741**, 19 (2008), astro-ph/0610440.
- [22] M. P. Hertzberg, M. Tegmark, and F. Wilczek, *Phys. Rev. D* **78**, 083507 (2008), 0807.1726.
- [23] S. De Panfilis, A. C. Melissinos, B. E. Moskowitz, J. T. Rogers, Y. K. Semertzidis, W. Wuensch, H. J. Halama, A. G. Prodell, W. B. Fowler, and F. A. Nezrick, *Phys. Rev. Lett.* **59**, 839 (1987).
- [24] C. Hagmann, P. Sikivie, N. S. Sullivan, and D. B. Tanner, *Phys. Rev. D* **42**, 1297 (1990).
- [25] Y. Kahn, B. R. Safdi, and J. Thaler, *Phys. Rev. Lett.* **117**, 141801 (2016), 1602.01086.

[26] A. Caldwell, G. Dvali, B. Majorovits, A. Millar, G. Raffelt, J. Redondo, O. Reimann, F. Simon, and F. Steffen (MADMAX Working Group), *Phys. Rev. Lett.* **118**, 091801 (2017), 1611.05865.

[27] L. Zhong et al. (HAYSTAC), *Phys. Rev. D* **97**, 092001 (2018), 1803.03690.

[28] D. J. E. Marsh, K.-C. Fong, E. W. Lentz, L. Smejkal, and M. N. Ali, *Phys. Rev. Lett.* **123**, 121601 (2019), 1807.08810.

[29] J. Schütte-Engel, D. J. E. Marsh, A. J. Millar, A. Sekine, F. Chadha-Day, S. Hoof, M. N. Ali, K.-C. Fong, E. Hardy, and L. Šmejkal, *JCAP* **08**, 066 (2021), 2102.05366.

[30] C. Bartram et al. (ADMX), *Phys. Rev. Lett.* **127**, 261803 (2021), 2110.06096.

[31] F. Wilczek, *Phys. Rev. Lett.* **58**, 1799 (1987).

[32] A. M. Essin, J. E. Moore, and D. Vanderbilt, *Phys. Rev. Lett.* **102**, 146805 (2009), 0810.2998.

[33] R. Li, J. Wang, X. Qi, and S.-C. Zhang, *Nature Phys.* **6**, 284 (2010), 0908.1537.

[34] D. Xiao et al., *Phys. Rev. Lett.* **120**, 056801 (2018), 1710.00471.

[35] A. Bermudez, L. Mazza, M. Rizzi, N. Goldman, M. Lewenstein, and M. A. Martin-Delgado, *Phys. Rev. Lett.* **105**, 190404 (2010), URL <https://link.aps.org/doi/10.1103/PhysRevLett.105.190404>.

[36] D. M. Nenno, C. A. C. Garcia, J. Gooth, C. Felser, and P. Narang, *Nature Rev. Phys.* **2**, 682 (2020).

[37] P. Sikivie, *Phys. Rev. Lett.* **51**, 1415 (1983), [Erratum: *Phys. Rev. Lett.* 52, 695 (1984)].

[38] R. H. Brown and R. Q. Twiss, *Nature* **177**, 27 (1956).

[39] URL <https://www.lownoisefactory.com/products/>.

[40] M. Hatridge, R. Vijay, D. H. Slichter, J. Clarke, and I. Siddiqi, *Physical Review B* **83** (2011), ISSN 1550-235X, URL <http://dx.doi.org/10.1103/PhysRevB.83.134501>.

[41] E. P. Menzel, F. Deppe, M. Mariantoni, M. . Araque Caballero, A. Baust, T. Niemczyk, E. Hoffmann, A. Marx, E. Solano, and R. Gross, *Physical Review Letters* **105** (2010), ISSN 1079-7114, URL <http://dx.doi.org/10.1103/PhysRevLett.105.100401>.

[42] D. Bozyigit, C. Lang, L. Steffen, J. Fink, C. Eichler, M. Baur, R. Bianchetti, P. Leek, S. Filipp, M. da Silva, et al., *Nature Phys* **7**, 154 (2011).

[43] Z. H. Peng, S. E. de Graaf, J. S. Tsai, and O. V. Astafiev, *Nature Communications* **7** (2016), ISSN 2041-1723, URL <http://dx.doi.org/10.1038/ncomms12588>.

[44] Y. Zhou, Z. Peng, Y. Horiuchi, O. Astafiev, and J. Tsai, *Physical Review Applied* **13** (2020), ISSN 2331-7019, URL <http://dx.doi.org/10.1103/PhysRevApplied.13.034007>.

- [45] P. Sikivie, Phys. Rev. D **32**, 2988 (1985), [Erratum: Phys. Rev. D 36, 974 (1987)].
- [46] M. Beutter, A. Pargner, T. Schwetz, and E. Todarello, JCAP **02**, 026 (2019), 1812.05487.
- [47] P. Sikivie, Phys. Lett. B **567**, 1 (2003), astro-ph/0109296.
- [48] C. Armendariz-Picon and J. T. Neelakanta, JCAP **03**, 049 (2014), 1309.6971.
- [49] A. Blais, A. L. Grimsmo, S. M. Girvin, and A. Wallraff, Rev. Mod. Phys. **93**, 025005 (2021), 2005.12667.
- [50] C. Bartram et al. (2021), 2110.10262.
- [51] D. Alesini et al., Phys. Rev. D **103**, 102004 (2021), 2012.09498.
- [52] C. M. Caves, Phys. Rev. D **26**, 1817 (1982), URL <https://link.aps.org/doi/10.1103/PhysRevD.26.1817>.
- [53] C. Macklin, K. O'Brien, D. Hover, M. E. Schwartz, V. Bolkhovsky, X. Zhang, W. D. Oliver, and I. Siddiqi, Science **350**, 307 (2015), URL <http://www.sciencemag.org/content/350/6258/307.abstract>.
- [54] C. Eichler, J. Mlynek, J. Butscher, P. Kurpiers, K. Hammerer, T. Osborne, and A. Wallraff, Physical Review X **5** (2015), ISSN 2160-3308, URL <http://dx.doi.org/10.1103/PhysRevX.5.041044>.
- [55] M. P. da Silva, D. Bozyigit, A. Wallraff, and A. Blais, Phys. Rev. A **82**, 043804 (2010), URL <http://link.aps.org/doi/10.1103/PhysRevA.82.043804>.
- [56] K. M. Backes, D. A. Palken, S. A. Kenany, B. M. Brubaker, S. B. Cahn, A. Droster, G. C. Hilton, S. Ghosh, H. Jackson, S. K. Lamoreaux, et al., Nature **590**, 238–242 (2021), ISSN 1476-4687, URL <http://dx.doi.org/10.1038/s41586-021-03226-7>.
- [57] A. Pankratov, L. Revin, A. Gordeeva, A. Yablokov, L. Kuzmin, and E. Il'ichev, npj Quantum Inf **8**, 61 (2022).

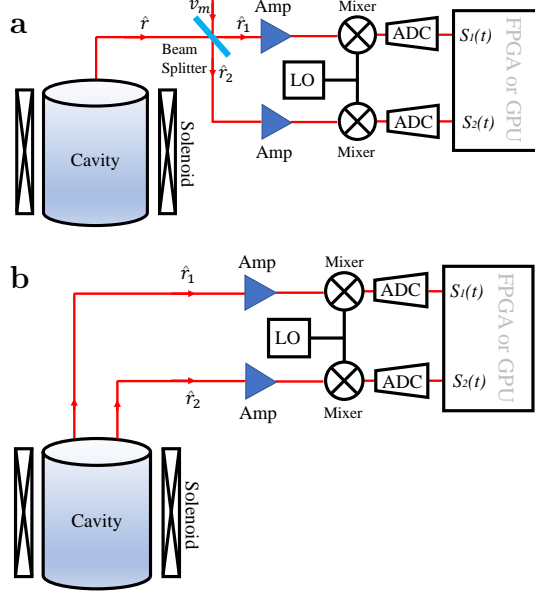


FIG. 1: The scheme of quantum dual-path setup for resonant cavity dark matter axions search.

(a) Single-sided cavity scheme. There is only one output port of the cavity detector. Axions convert to microwave single-photons that escape from the cavity as a propagation quantum field with annihilation operator \hat{r} , subsequently passes through a 50/50 beam splitter along with vacuum field or weak thermal field \hat{v}_m near cavity at 20 mK stage in a refrigerator. The output fields \hat{r}_1 and \hat{r}_2 are then amplified by two nominally identical amplification chains (denotes as AMP) and down-converted into intermediate (e.g. 25 MHz) frequency ω_{if} with a mixer by the local oscillator (LO) at the same frequency as the cavity's resonance frequency. The field quadratures are recorded by analog-to-digital converters (ADCs), the complex envelopes S_i are then extracted and calculated by FPGA or GPU electronics in real time. The single-sided cavity scheme can overcome the inevitable insertion loss between the beam splitter and the AMP. (b) Two-sided cavity scheme. If there are two identical output ports of the cavity detector, the converted microwave single-photons escape from the two output ports with equal probability and the beam-splitter is not necessary. The correlations between the two cavity outputs behave like to the outputs of the beam splitter in (a). However, it is expected the SNR in this scheme is even higher than the scheme described in (a). It can overcome the inevitable insertion loss between the cavity and the AMP.

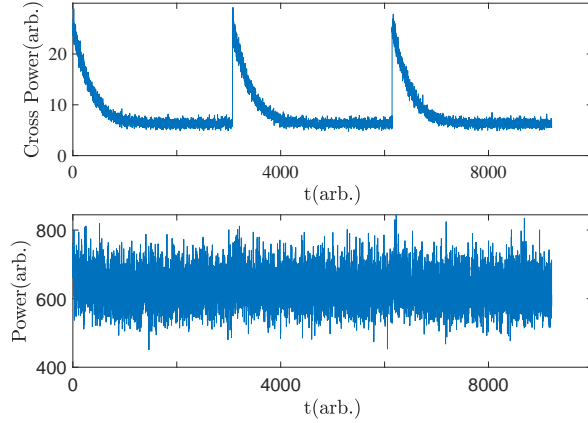


FIG. 2: Illustrative comparison between simulated cross power (upper) and single-channel power (lower). A periodical signal is injected with white noise. The signal to noise ratio is about a hundred times higher when using the cross power setup that reveals the injected signal.

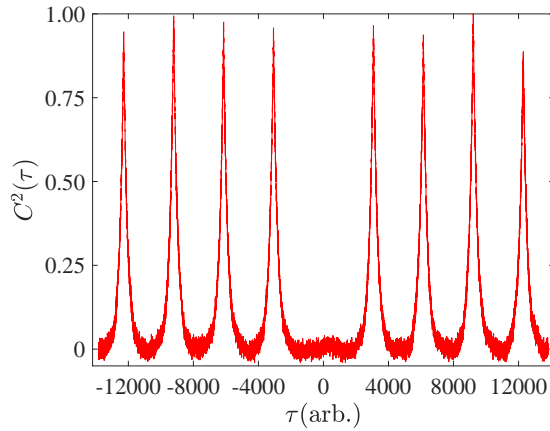


FIG. 3: The simulation of the second order correlation function measurement for single-photon pulse train with white noise. If photon antibunching observed in experiment as $C^2(0) < C^2(\tau)$, the converted periodic signal is non-classical.